

Multidirectional available high-frequency response with zero-field resonance above 8 GHz in epitaxial α -Fe(001) films

This content has been downloaded from IOPscience. Please scroll down to see the full text.

2015 Appl. Phys. Express 8 053001

(<http://iopscience.iop.org/1882-0786/8/5/053001>)

View [the table of contents for this issue](#), or go to the [journal homepage](#) for more

Download details:

IP Address: 192.236.36.29

This content was downloaded on 13/04/2015 at 01:31

Please note that [terms and conditions apply](#).

Multidirectional available high-frequency response with zero-field resonance above 8 GHz in epitaxial α -Fe(001) films

Cunxu Gao[†], Yutian Wang^{*†}, Chengyi Li, Yanping Wei, Zhendong Chen, Guozhi Chai, and Desheng Xue*

Key Lab for Magnetism and Magnetic Materials of the Ministry of Education, Lanzhou University, Lanzhou 730000, P. R. China

E-mail: wangyt08@lzu.edu.cn; xueds@lzu.edu.cn

Received January 26, 2015; accepted March 18, 2015; published online April 7, 2015

We investigate the high-frequency characteristics of epitaxial single crystal α -Fe(001) thin films by permeability spectroscopy with microwave transmission along different in-plane crystal directions. The results show an in-plane isotropic static permeability above 50 with a multidirectional zero-field resonance frequency (f_r) higher than 8 GHz in the films. We demonstrate that these multidirectional available high-frequency characteristics result from the strong magnetocrystalline anisotropy in the films and not from other kinds of magnetic anisotropies. The study on thickness-dependent films show f_r being stable at 8.4 GHz in the films thicker than about 20 nm. © 2015 The Japan Society of Applied Physics

Magnetic materials with a high permeability have been extensively utilized in many high-frequency applications such as microwave noise filters, thin-film inductors and so on.^{1–8)} As the operating frequency in many modern devices reaches the gigahertz range, various magnetic thin films with a high resonance frequency f_r (above 6 GHz)^{6–11)} have been developed by employing their in-plane uniaxial magnetic anisotropy¹⁰⁾ or unidirectional anisotropy.¹¹⁾ However, optimal high-frequency characteristics can only be approached under the condition that the microwave magnetic field is perpendicular to the unique easy axis for such kind of magnetic anisotropy.^{10–12)} A possible solution to generate an isotropic response is using rotatable magnetic anisotropy, which was reported in several studies.^{13,14)} Although the rotatable magnetic anisotropy can result in an isotropic zero-field resonance with a frequency as high as 4.5 GHz,⁷⁾ it is hard to keep a high permeability with concomitant stripe domains arising, and sensitive to the thickness and temperature of the films; thus, it is confronting disadvantages for applications.^{7,13,14)} Consequently, magnetic materials with a multidirectional available high permeability and high resonance frequency remain in persistent demand for high-frequency applications.

Nonunique stable directions of magnetization were considered to be an important condition to realize multidirectional high-frequency resonance in magnetic films. Single-crystal α -Fe films have exhibited the expected fourfold magnetic anisotropy,¹⁵⁾ high saturation magnetization ($4\pi M_s = 2.1$ T), and normally small coercivity field (H_c lower than 20 Oe), which are expected to be an ideal system to investigate multidirectional high-frequency characteristics.

In the present work, we epitaxially grew thickness-dependent α -Fe films on a GaAs(001) substrate and studied their high-frequency characteristics. We found that a multidirectional high-frequency resonance could be generated by employing its in-plane fourfold magnetocrystalline anisotropy in the films, which can result in a multidirectional frequency f_r higher than 8 GHz. The nonunique stable directions of magnetization in the films were discussed to understand the mechanism.

The epitaxial growth of Fe films was performed in a custom-built molecular-beam epitaxy (MBE) system equipped with a solid-source effusion cell for Fe. Nucleation and growth were monitored in situ by reflection high-energy

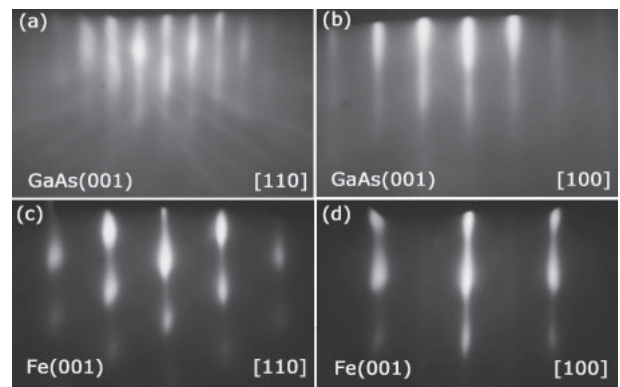


Fig. 1. RHEED patterns of a GaAs(001) substrate and the Fe(001) films grown on it. The electron beam is along the in-plane directions of [100] and [110].

electron diffraction (RHEED). A substrate temperature of 50 °C was chosen to avoid interfacial reactions between Fe and GaAs. The thicknesses of the Fe films were determined by a calibrated growth rate of 0.14 nm/min. All films were capped with a 3-nm-thick Al layer and exhibit a root-mean-square roughness less than 1 nm, as measured by atomic force microscopy over an area of $5 \times 5 \mu\text{m}^2$. The surface steps observed in the micrographs have no preferential orientation, as we have used singular (on-axis) substrates ($\pm 0.5^\circ$). A vibrating sample magnetometer (VSM) was used for the measurement of the angular-dependent remanence curves and hysteresis loops at room temperature.¹⁶⁾ All magnetization data presented in the following were corrected for the diamagnetic background of the substrate. The microwave permeability measurements along different in-plane crystal directions of the Fe films were carried out with a PNA E8363B vector network analyzer (VNA) by using the shorted microstrip method from 100 MHz to 15 GHz with a microwave power of -12 dBm. During the measurement, a very thin sample holder with angular marks attached to the film was plugged into the shorted microstrip line fixture that is connected to the VNA.^{7,17,18)}

The RHEED patterns were taken before and after Fe growth at different azimuths for clarifying the crystal directions.^{15,19)} Figures 1(a) and 1(b) show the familiar stationary RHEED patterns of the GaAs(001) surface taken along the $\langle 110 \rangle$ and $\langle 100 \rangle$ azimuths, respectively, prior to Fe growth. Figures 1(c) and 1(d) show the RHEED patterns of the Fe surface taken along the $\langle 110 \rangle$ and $\langle 100 \rangle$ azimuths of GaAs,

[†]These authors contributed equally to this work.

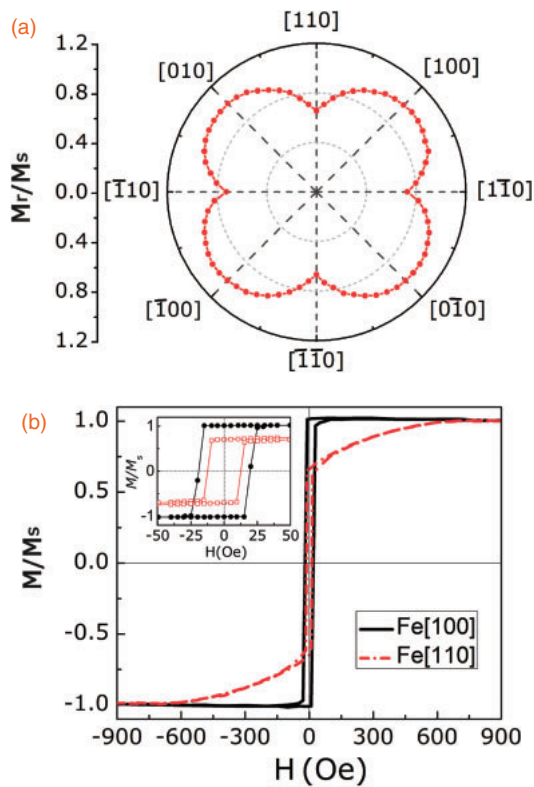


Fig. 2. (a) Polar plots of the in-plane angular dependent magnetic remanence (M_r) for the 26-nm-thick Fe(001) films. (b) The hysteresis loops with a magnetic field applied along the Fe[100] and Fe[110] directions for the same sample. The inset shows a magnification of the low-magnetic-field range measured along Fe[100] (solid circle) and Fe[110] (open square) directions, respectively.

respectively, with an Fe film grown to a thickness of 10 nm. The stationary RHEED patterns evidence an epitaxial and smooth film but exhibit the reflections of different lattice plane distances indicating the fact that the GaAs lattice constant is almost twice that of α -Fe and directly revealing an orientation relationship between Fe and GaAs(001), i.e., α -Fe(001) $\langle 100 \rangle \parallel$ GaAs(001) $\langle 100 \rangle$.

As a typical epitaxial single-crystal heterostructure, cubic magnetocrystalline anisotropy has been proven to be dominant against interface anisotropy in α -Fe films on GaAs(001) with a thickness greater than 20 nm.^{20,21} Considering the strong demagnetizing field perpendicular to the films and no extra perpendicular magnetic anisotropies existing, the magnetization remains parallel to the surface of the films for all samples we investigated in this work.²² The angular-dependent magnetic remanence (M_r) was measured by a VSM to study the in-plane symmetry of the magnetic anisotropy. Figure 2(a) shows its polar plots for 26-nm-thick Fe films. It can be clearly seen from Fig. 2(a) that the two easy axes of magnetization in the [100] and [010] directions evidence the expected in-plane fourfold anisotropy. Figure 2(b) shows the in-plane hysteresis loops measured with a magnetic field applied along the Fe[100] and Fe[110] directions. The in-plane hysteresis loops measured along the Fe[110] direction (45° rotation with respect to the easy axes) exhibit a residual magnetization ratio (M_r/M_s) of about 0.7, which can be explained by M_s projected with an angle of 45°, i.e., $M_r = M_s \cos(\pi/4)$. A magnetic anisotropy field (H_k) of 605 Oe and a coercivity field (H_c) lower than 20 Oe in both

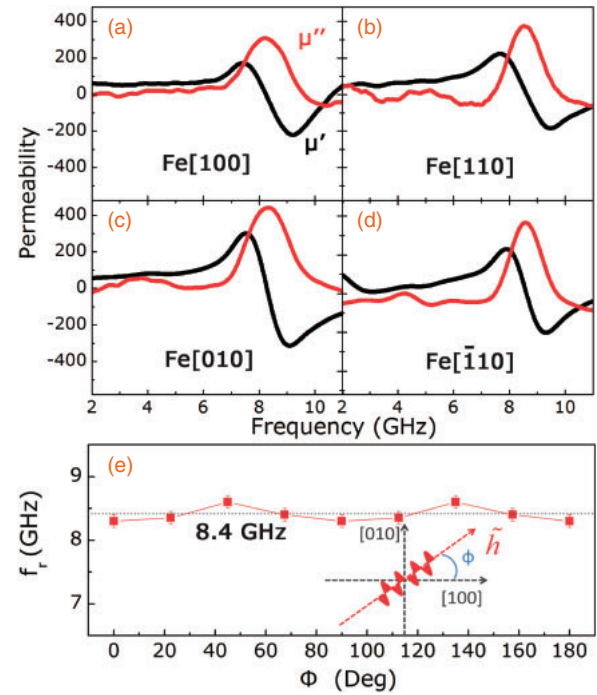


Fig. 3. High-frequency permeability spectra of the 26-nm-thick Fe(001) films with in-plane microwave transmission along the (a) [100], (b) [110], (c) [010], and (d) $\bar{1}10$ directions of the Fe films. (e) In-plane angular dependence of f_r on the angle Φ , schematically shown in the inset depicting the angle between the microwave transmission direction and Fe[100].

the [100] and [110] directions can be obtained from the hysteresis loops shown in Fig. 2(b).

The hysteresis loops measured in the Fe[100] and Fe[010] directions show square shapes, indicating the magnetization can be stable in both directions. Because Fe[100] and Fe[010] are two easy axes and perpendicular to each other, the projection of the magnetization in any in-plane azimuth cannot be zero. Based on this feature of the sample, the angular dependencies of the high-frequency permeability spectra were measured and studied. Figures 3(a)–3(d) show the permeability spectra of the 26-nm-thick Fe(001) films with microwave transmission along different crystal directions. Prior to measurement in every direction, a strong DC field of 3000 Oe was applied to saturate the magnetization for 5 s, followed by a decrease in the field to zero. A static permeability μ_s above 50 and a resonance frequency f_r higher than 8 GHz were achieved. The unstable permeability obtained in Figs. 3(b)–3(d) is considered to result from the nonuniform alignment of the magnetic structure in the remanence magnetization state when saturated along nonstrict easy axis.²³ The in-plane angular dependence of f_r on the angle Φ between the microwave transmission direction and Fe[100] shown in Fig. 3(e) demonstrates that the zero-field resonances are isotropic with a fitting frequency value of 8.4 GHz, which usually cannot occur in a system with an in-plane uniaxial magnetic anisotropy.¹²

Classically, the magnetization dynamics under microwave excitation can be theoretically described by the Landau–Lifshitz–Gilbert equation.²⁴ The high resonance frequency can be obtained by combining Landau–Lifshitz–Gilbert equation and the free energy density F in our films written without an applied field as²⁵

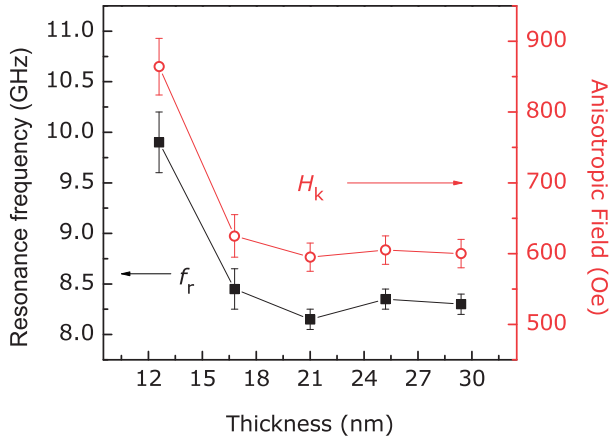


Fig. 4. Experimental results of the resonance frequency f_r and magnetic anisotropy field H_k of thickness-dependent Fe films.

$$F = -2\pi M_s^2 \sin^2 \theta + \frac{K_u}{t} \sin^2 \theta \cos^2(\varphi - \varphi_u) - \frac{1}{8} K_1 (3 + \cos 4\varphi) \sin^4 \theta, \quad (1)$$

where θ is the polar angle of M_s with respect to the out-of-plane axis (i.e., Fe[001]), φ is the azimuthal angle between the projection of M_s onto the sample surface and the in-plane easy axis, K_u is the interface-induced in-plane uniaxial anisotropy constant, K_1 is the cubic anisotropy constant, t is the thickness of the films, and φ_u is the angle between the easy axes of the interface and the magnetocrystalline anisotropies. Considering the case in which $\varphi_u = 45^\circ$ in the Fe/GaAs(001) system²⁰ and M_s lies strictly within the film plane (i.e., $\theta = 90^\circ$), the resulting zero-field resonance frequency can be written as

$$f_r = \frac{\gamma}{2\pi} \left[4\pi M_s + \frac{2K_u}{Mt} \cos^2 \varphi + \frac{K_1}{2M} (3 + \cos 4\varphi) \right]^{1/2} \times \left(\frac{2K_u}{Mt} \cos 2\varphi + \frac{2K_1}{M} \cos 4\varphi \right)^{1/2}. \quad (2)$$

Comparing Eq. (2) with the equation of $f_r = \gamma/2\pi[(4\pi M_s + H_k)H_k]^{1/2}$ obtained by setting the stable equilibrium condition of φ using $\partial F/\partial \varphi = 0$,²⁶ the magnetic field $H_k = 2K_u/Mt + 2K_1/M$, which is determined by the thickness-dependent uniaxial anisotropy and constant cubic magnetocrystalline anisotropy. In order to evidence that the high f_r results from the magnetocrystalline anisotropy, the measurements were taken for Fe films with different thicknesses. As shown in Fig. 4, the thickness-dependent H_k and f_r follow the relations obtained above, which show the trend to a constant value with increasing film thickness for each of them. Consequently, H_k and f_r stabilize at 600 Oe and 8.4 GHz, respectively, for the Fe films thicker than about 20 nm.

In conclusion, we report multidirectional available high-frequency characteristics in epitaxial single-crystal α -Fe(001)

films. The isotropic zero-field f_r driven by the magneto-crystalline anisotropy and not by other kinds of magnetic anisotropies approaches a higher range above 8.4 GHz. Our investigation shows single-crystal ferromagnetic films for high-frequency applications by using its strong magneto-crystalline anisotropy, which leads to interesting characteristics and a conceivable advantage for applications.

Acknowledgments This work was supported by the National Basic Research Program of China (Grant No. 2012CB933101), the National Natural Science Foundation of China (Grant Nos. 11274147, 53171093, and 51471080), and the Fundamental Research Funds for the Central Universities (Grant Nos. lzujbky-2013-ct01 and lzujbky-2014-40).

- 1) S. X. Wang, N. X. Sun, M. Yamaguchi, and S. Yabukami, *Nature* **407**, 150 (2000).
- 2) N. D. Ha, M. H. Phan, and C. O. Kim, *Nanotechnology* **18**, 155705 (2007).
- 3) R. C. Che, L.-M. Peng, X. F. Duan, Q. Chen, and X. L. Liang, *Adv. Mater.* **16**, 401 (2004).
- 4) L. P. Carignan, V. Boucher, T. Kodera, C. Caloz, A. Yelon, and D. Ménard, *Appl. Phys. Lett.* **95**, 062504 (2009).
- 5) G. Lu, H. Zhang, J. Q. Xiao, X. Tang, Y. Xie, and Z. Zhong, *J. Appl. Phys.* **109**, 07A308 (2011).
- 6) G. Z. Chai, Y. C. Yang, J. Y. Zhu, M. Lin, W. B. Sui, D. W. Guo, X. L. Li, and D. S. Xue, *Appl. Phys. Lett.* **96**, 012505 (2010).
- 7) G. Z. Chai, N. N. Phuoc, and C. K. Ong, *Appl. Phys. Lett.* **103**, 042412 (2013).
- 8) H. W. Chang, L. C. Chuang, C. W. Shih, W. C. Chang, and D. S. Xue, *J. Appl. Phys.* **115**, 17A312 (2014).
- 9) N.-N. Song, H.-T. Yang, H.-L. Liu, X. Ren, H.-F. Ding, X.-Q. Zhang, and Z.-H. Cheng, *Sci. Rep.* **3**, 3161 (2013).
- 10) X. L. Fan, D. S. Xue, M. Lin, Z. M. Zhang, D. W. Guo, C. J. Jiang, and J. Q. Wei, *Appl. Phys. Lett.* **92**, 222505 (2008).
- 11) N. N. Phuoc, W. T. Soh, G. Z. Chai, and C. K. Ong, *J. Appl. Phys.* **113**, 073902 (2013).
- 12) L. T. Hung, N. N. Phuoc, and C. K. Ong, *J. Appl. Phys.* **106**, 063907 (2009).
- 13) G. Z. Chai, N. N. Phuoc, and C. K. Ong, *Sci. Rep.* **2**, 832 (2012).
- 14) S. Tacchi, S. Fin, G. Carlotti, G. Gubbiotti, M. Madami, M. Barturen, M. Marangolo, M. Eddrief, D. Bisero, A. Rettori, and M. G. Pini, *Phys. Rev. B* **89**, 024411 (2014).
- 15) J. J. Krebs, B. T. Jonker, and G. A. Prinz, *J. Appl. Phys.* **61**, 2596 (1987).
- 16) X. L. Fan, D. S. Xue, C. J. Jiang, Y. Gong, and J. Y. Li, *J. Appl. Phys.* **102**, 123901 (2007).
- 17) V. Bekker, K. Seemann, and H. Leiste, *J. Magn. Magn. Mater.* **270**, 327 (2004).
- 18) J. W. Wei, J. B. Wang, Q. F. Liu, X. Y. Li, D. R. Cao, and X. J. Sun, *Rev. Sci. Instrum.* **85**, 054705 (2014).
- 19) C. X. Gao, H. P. Schönherr, and O. Brandt, *Appl. Phys. Lett.* **97**, 031906 (2010).
- 20) O. Thomas, Q. Shen, P. Schieffer, N. Tournerie, and B. Lépine, *Phys. Rev. Lett.* **90**, 017205 (2003).
- 21) G. Bayreuther, J. Prempfer, M. Sperl, and D. Sander, *Phys. Rev. B* **86**, 054418 (2012).
- 22) Y. T. Wang, F. Z. Lv, O. Brandt, J. Herfort, C. X. Gao, and D. S. Xue, *Ann. Phys.* **526**, L1 (2014).
- 23) E. Gu, J. A. C. Bland, C. Daboo, M. Gester, L. M. Brown, R. Ploessl, and J. N. Chapman, *Phys. Rev. B* **51**, 3596 (1995).
- 24) L. D. Landau and E. M. Lifshitz, *Phys. Z. Sowjetunion* **8**, 153 (1935).
- 25) K. Lenz, E. Kosubek, K. Baberschke, H. Wende, J. Herfort, H. P. Schönherr, and K. H. Ploog, *Phys. Rev. B* **72**, 144411 (2005).
- 26) X. L. Fan, W. Wang, Y. T. Wang, H. A. Zhou, J. W. Rao, X. B. Zhao, C. X. Gao, Y. S. Gui, C. M. Hu, and D. S. Xue, *Appl. Phys. Lett.* **105**, 262404 (2014).